Research in Astronomy and Astrophysics, 25:025008 (10pp), 2025 February

https://doi.org/10.1088/1674-4527/ada74e
CSTR: 32081.14.RAA.ada74e

LAMOST Medium-resolution Spectroscopic Survey of Galactic Open Clusters (LAMOST-MRS-O): An Overview of Survey Plan and Preliminary Results

Xi Zhang (张茜)[1,2,3,4], Chengzhi Liu (刘承志)[1], Jing Zhong (钟靖)[3], Li Chen (陈力)[2,3], Ali Luo (罗阿理)[5], Jianrong Shi (施建荣)[5], Chao Liu (刘超)[5], Jianjun Chen (陈建军)[5], Haotong Zhang (张昊彤)[5], Jinliang Hou (侯金良)[2,3]LAMOST MRS Collaboration
[1] Changchun Observatory, National Astronomical Observatories, Chinese Academy of Sciences, Changchun 130117, China
[2] School of Astronomy and Space Science, University of Chinese Academy of Sciences, Beijing 100049, China; chenli@shao.ac.cn
[3] Astrophysics Division, Shanghai Astronomical Observatory, Chinese Academy of Sciences, Shanghai 200030, China; jzhong@shao.ac.cn
[4] Institute of Astronomy and Information, Dali University, Dali 671003, China
[5] CAS Key Laboratory of Optical Astronomy, National Astronomical Observatories, Chinese Academy of Sciences, Beijing 100101, China
Received 2024 December 12; revised 2024 December 31; accepted 2025 January 3; published 2025 January 29

Abstract

As part of the LAMOST medium-resolution spectroscopic survey, the LAMOST-MRS-O is a non-time domain survey that aims to perform medium-resolution spectral observations for member stars in the open cluster areas. This survey plans to obtain the spectroscopic parameters such as radial velocity and metal abundances of member stars and provide data support for further study on the chemical and dynamical characteristics and evolution of open clusters in combination with Gaia data. We have completed the observations on ten open cluster fields and obtained 235184 medium-resolution spectra of 133792 stars. Based on the data analyzed of LAMOST DR11v1.1, for some clusters of particular concern, it is found that the sampling ratio of members stars with Gmag < 15 mag can reach 70%, which indicates that the LAMOST-MRS-O has reached our initial design goal.

Key words: (Galaxy:) open clusters and associations: general – techniques: spectroscopic – surveys

1. Introduction

The single-stellar-population origin of open clusters makes its member stars share many similar physical characteristics (such as age, distance, velocity, abundance, etc.). The cluster members include stars at various stages of evolution, such as various types of variable stars, binary stars, and stars with special astrophysical significance, e.g., hot subdwarfs (Luo et al. 2019), blue straggler stars (Li et al. 2023, 2024), red clump stars (Bragaglia et al. 2001), etc. Open star clusters have become an ideal test place for the evolution theory of stars and binaries and provide crucial constraints for the stellar formation and evolution models.

Due to the wide age distribution (throughout the formation history of the Galactic disk) and mass distribution (from hundreds to tens of thousands of solar masses) of the open clusters, the detailed study of the properties of large sample open cluster members, such as the ratio of binary stars and their mass ratio distribution (Li & Shao 2022), mass function (Jiang et al. 2024), and mass segregation (Chen et al. 2007), will further increase our understanding of the formation and evolution of the stellar system (Könyves et al. 2015; André et al. 2019).

Since the release of Gaia DR2 data in 2018 (Gaia Collaboration et al. 2018), high-precision astrometry and photometry data have significantly improved the reliability of the determination results of open cluster members, thus extensively promoting the open cluster study. In addition, spectroscopic observation can provide more physical information about member stars, such as radial velocity, atmospheric parameters, element abundance, rotation velocity etc., (Donor et al. 2020; Zhong et al. 2020; Fu et al. 2022). This information is also essential to better study the nature of open clusters and their member stars.

The LAMOST low-resolution spectroscopic survey (LAMOST-LRS) was officially started in 2012. It has obtained more than 20 million spectra and has a significant sky coverage (especially in the region of the Galactic-anti center). It has carried out uniform sampling and observation of a large number of star targets on the Galactic disk, including many open star clusters. (Zhong et al. 2020) obtained the mean values of radial velocity and metallicity of 295 open clusters using the LAMOST low-resolution spectra (DR5). Using these clusters as a tracer, combined with the Gaia DR2 data, the radial and vertical metallicity gradients of the Galactic disk and their changes with age were studied. Furthermore, (Fu et al. 2022) used LAMOST low-resolution spectra (DR8) and Gaia data to provide a catalog containing property parameters of 386 cluster and studied the abundance distribution of the Galaxy and the dynamic properties of the Galactic disk.

The LAMOST medium-resolution spectroscopic survey (LAMOST-MRS), officially started in 2018 September, has a

spectral resolution of $R \sim 7500$ and wavelength coverage of 4950 Å–5350 Å at the blue part and 6300 Å–6800 Å at the red part. The LAMOST medium-resolution stellar spectrum can obtain nearly 20 chemical elements, such as lithium, carbon, sodium, magnesium, silicon, calcium, iron, manganese, nickel, etc., and the radial velocity with accuracy reached to nearly $1\,\mathrm{km\,s^{-1}}$ (Liu et al. 2020).

As one of the LAMOST-MRS survey projects, LAMOST-MRS-O adopts multiple-visit observational modes with the same plate pointing but different fiber positions for the open cluster fields. This mode allows one to observe as many different cluster members as possible, improving the sampling rate of cluster member stars. LAMOST-MRS-O, obtaining the medium-resolution spectra of member stars, can provide radial velocity, atmospheric parameters, and element abundance more accurately than the low-resolution LAMOST spectra observed before. Furthermore, the LAMOST-MRS-O project aims to obtain a sample of cluster member spectra ($G\mathrm{mag} = 9$–15 mag) with higher completeness, which will provide very important data support for studying the cluster properties and the stellar formation and evolution.

This paper mainly introduces the LAMOST-MRS-O spectroscopic survey project, including its scientific objectives, observing property parameters, and observed data qualities.

2. LAMOST-MRS-O Survey

LAMOST can simultaneously obtain spectral information of about 4000 sources and has unique advantages as large samples of spectroscopic surveys. However, for the specific observation of the open cluster field, according to the analysis of the results of LAMOST low-resolution survey data (DR5), the average sampling density in the low Galactic Latitude (b) region($-10^\circ < b < 10^\circ$) is about $280\,\mathrm{stars\,deg^{-2}}$. Due to the nearly uniform optical fiber distribution in the LAMOST focal plate, the sampled number of stars within the half number radius of most open clusters (with an average scale of about ten arc-minutes) is only about ten (Zhong et al. 2020). The low sampling rate of member stars will seriously restrict the relevant cluster research work.

To solve the above problems, in 2018 September, the LAMOST-MRS launched a sub-project of the open cluster observation (LAMOST-MRS-O). The observation magnitude range is from $G\mathrm{mag} = 9$–15 mag, and the sampling density of member stars can reach about 1000–2000 $\mathrm{deg^{-2}}$. Considering that the optical fiber density of LAMOST is $200\,\mathrm{deg^{-2}}$, it is planned to adopt the multiple-visit mode for different member stars in the same cluster field. For each field, the total number of visits will be no less than eight, so the total number of observed member stars in the cluster area (about ten arc-minutes) is expected to be over 50. Based on this observation scheme, the statistical analysis of the cluster properties will be significantly improved. At the same time, under the LAMOST multiple-visit observation mode, some stars inevitably undergo repeated observations in the star cluster field. This will also provide valuable data for studying the time-domain properties of cluster members and field stars.

Compared with the LAMOST low-resolution spectrum, the LAMOST medium-resolution spectrum is expected to obtain more element abundances and stellar atmospheric parameters with higher accuracy. For example, under the condition of S/N greater than 10, the precision of radial velocity is about $1\,\mathrm{km\,s^{-1}}$, [Fe/H] about 0.06 dex, other element abundance about 0.06–0.12 dex, stellar surface gravity about 0.17 dex and effective temperature about 110 K (Wang et al. 2020).

2.1. Scientific Goals

In recent years, more and more open clusters have been discovered by using high-precision Gaia astrometry and photometric data (Bica et al. 2019; Liu & Pang 2019; Cantat-Gaudin et al. 2020; Castro-Ginard et al. 2021; He et al. 2021; Qin et al. 2021, 2023; He et al. 2022; Hunt & Reffert 2023, 2024). The number of star clusters has been greatly expanded. As the reliability and completeness of identifying open cluster members improves, an increasing number of clusters have been observed to exhibit tidal tail structures (Carrera et al. 2019; Röser & Schilbach 2019; Röser et al. 2019; Zhang et al. 2020; Bai et al. 2022) and even the original extended structure (Zhong et al. 2019). In particular, in addition to having a much-extended region than before, it was found that the radial density distribution of a large portion of open clusters can be represented by a two-component distribution, which indicates that the extended structure of open clusters is not just a simple extension of the core components, but may have different origin or dynamical evolution characteristics. (Zhong et al. 2022). These new understandings and discoveries of star clusters require more observations and in-depth research.

Combined with Gaia data, the LAMOST-MRS-O project will observe more cluster member spectra and obtain the radial velocity and atmospheric parameters of member stars, such as temperature, surface gravity, chemical abundance, etc., which will provide a unique contribution to a comprehensive understanding of the physical properties of cluster member stars. Furthermore, based on the three-dimensional velocity, spatial distribution, and chemical abundance of member stars, one can also statistically study the dynamical disruption process (Odenkirchen et al. 2003), the cluster extended structure (Zhong et al. 2019; Bai et al. 2022), and the chemical evolution characteristic of star clusters (Zhong et al. 2020).

In addition, the LAMOST-MRS-O project may provide highly complete cluster member spectra for some clusters, especially in the outer region, which is of great scientific significance for the statistical study of various types of stars, such as Cepheid variable stars (Pietrukowicz et al. 2021; Hao et al. 2022; Lin et al. 2022), Be stars (Tarasov &

Table 1
The Plan of LAMOST-MRS-O Project Observation

Plan ID	Central Star	R.A. (2000)	Decl. (2000)	*N*star	*N*ocs	*N*_memb	Remark
NT002740+583314C	HIP 2191	00:27:40.51	+58:33:14.08	23927	8	992	Y
NT014347+555239C	HIP 8081	01:43:47.05	+55:52:39.11	25538	4	885	Y
NT014355+602612C	HD 10474	01:43:55.05	+60:26:12.23	24349	13	1315	...
NT021558+581737C	HD 13744	02:15:58.69	+58:17:37.00	24592	13	3186	Y
NT024142+552853C	HIP 12575	02:41:42.76	+55:28:53.76	18401	6	904	Y
NT024709+603414C	HIP 13004	02:47:09.67	+60:34:14.74	16096	20	1948	...
NT033932+592643C	HIP 17075	03:39:32.64	+59:26:43.51	11761	5	782	Y
NT041712+505156C	HIP 19986	04:17:12.30	+50:51:56.95	13220	9	767	Y
NT043052+443610C	HIP 21062	04:30:52.88	+44:36:10.98	13944	4	923	...
NT045451+440349C	HIP 22842	04:54:51.22	+44:03:39.56	18941	11	1446	Y
NT052826+344150C	HIP 25624	05:28:26.39	+34:41:50.93	20667	15	2961	Y
NT054955+314708C	HIP 27538	05:49:55.53	+31:47:08.66	23671	10	1616	...
NT061047+133934C	HIP 29310	06:10:47.36	+13:39:34.09	20206	18	1227	Y
NT061156+231225C	HIP 29425	06:11:56.25	+23:12:25.42	20727	13	2178	...
NT063435+045804C	HIP 31363	06:34:35.61	+04:58:04.87	21081	15	1801	Y
NT184324-054140C	HD 173005	18:43:24.07	-05:41:40.52	43882	19	3379	...
NT194619+222809C	HIP 97289	19:46:19.48	+22:28:09.95	22572	11	1209	...
NT200015+295514C	HIP 98460	20:00:15.53	+29:55:14.30	33955	9	1311	...

Note. This table provides details about the observation plan: "*N*star" refers to the number of all stars, while "*N*memb" represents the number of member stars in the open cluster that are planned for observation. The letter "Y" represents the area that has completed its observations up to now.

Malchenko 2012; Lin et al. 2015), blue straggler stars (Sindhu et al. 2018; Rain et al. 2020, 2021; Li et al. 2023, 2024), red clump stars (Chen et al. 2017, 2020; Magrini et al. 2021) and T Tauri stars (Preibisch et al. 2005; Maucó et al. 2018), etc. In particular, for some unique phenomena of stellar evolution in open clusters, such as lithium depletion (Smiljanic et al. 2010; Romano et al. 2021), extended main-sequence turn-offs (Li et al. 2019; Sun et al. 2019; He et al. 2023), etc., the measurement results of lithium abundance and stellar rotation velocity from the LAMOST medium-resolution spectra will provide significant data support for these studies.

2.2. Observation Plan and Strategy

In order to obtain a large number of spectra of cluster members in the LAMOST-MRS-O, we selected 18 open cluster related fields (hereafter OCs fields, as shown in Table 1). Each OCs field contains at least 4–5 open clusters, with a total of about 180 clusters (Cantat-Gaudin et al. 2018) (hereafter CG18) and 397356 stars (Gmag < 15 mag). Since most of the OCs are located in the Galactic plane, our 18 OCs fields are arranged on the low Galactic latitude, mainly distributed in the direction of the Galactic-anti center ($130^\circ < l < 240^\circ$, and $-10^\circ < b < 10^\circ$, where l, b represent the Galactic longitude and latitude respectively), ranging from 8 to 14 kpc from the Galactic center, with ages between 30 Myr and 1 Gyr, as shown in Figure 1. The overlap of each sky area shall not be greater than 10%. Based on 20 square degrees of each sky area, the coverage area of the LAMOST-MRS-O is about 360 square degrees.

The LAMOST-MRS-O project was launched in 2018 September and ended in 2023 June, lasting five years. The observed time in each year is from September of the current year to the middle of June of the following year. The LAMOST-MRS-O project is classified as a non-time-domain (hereafter NT) observation mode, which is arranged on a gray night. Since an NT survey does not use single-exposure information, we are able to co-add the single-exposure spectra for the same star to achieve higher S/N. Typically, a LAMOST-MRS-O plate will continuously take three single 1200 s exposures and obtain the co-added spectra with a total exposure time of 3×1200 s. This can obtain a limiting magnitude of $G = 14.5$ mag for the blue band and 15 mag for the red band with S/N ~ 10. In terms of observation strategy, aiming at improving the sampling rate of member stars as much as possible, the completeness of obtained cluster members will increase to 70% through eight plates of spectroscopic observations, down to $G = 15$ mag.

3. Survey Data

LAMOST DR11 v1.1 was released in 2024 September,[6] which included medium-resolution spectroscopy data from late 2018 October to 2023 June. The LAMOST DR11v1.1 provided over 10 million medium-resolution spectra, of which over 2.58 million spectra have atmospheric parameters. There are two kinds of stellar catalog present: the general catalog, which only includes general information including radial

[6] http://www.lamost.org/dr11/v1.1/

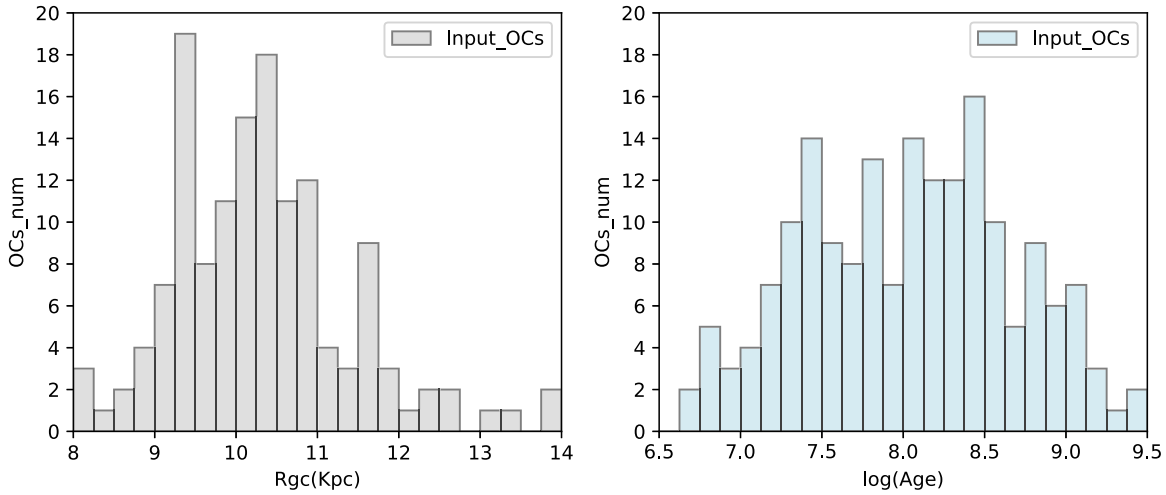

Figure 1. LAMOST-MRS-O Project plans to observe 18 cluster areas containing more than 180 clusters from CG18. Left panel: distribution of cluster distance from the Galactic center. Right panel: distribution of cluster ages in logarithm.

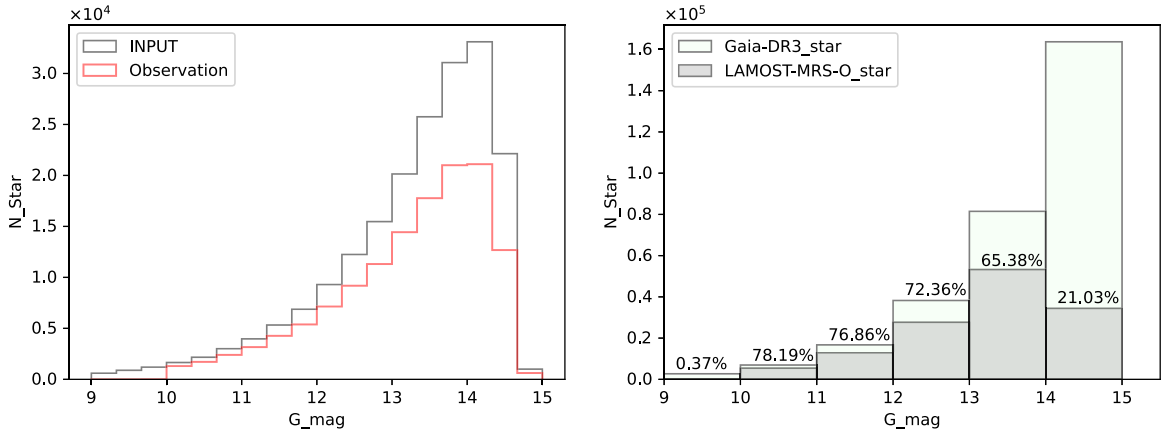

Figure 2. The left panel presents histograms of input stars (in gray) and observed stars (in red), wherein the observation rate is around 70% within the *G*mag range spanning from 9 to 15. The right panel shows the histogram of observed stars and their completeness rate within each magnitude bin in comparison to Gaia DR3. For stars with a magnitude ranging from 10 to 13 mag, the completeness rate of the observed stars can exceed 75%.

velocity parameter; the stellar parameter catalog, which additionally provides the atmospheric parameters and abundance of 13 different chemical elements.

In LAMOST DR11, ten OCs fields within the LAMOST-MRS-O project have finished the observational task. Specifically, each of these OCs fields has been observed with eight different spectroscopic plates. The general catalog encompasses 235,184 combined spectra of 133,792 stars distributed in ten cluster areas, with the spectra incorporating details about either the blue end or the red end, while the S/N for all spectra are greater than 5. Furthermore, the stellar parameter catalog contains 105,068 spectra of 67,318 stars in the same cluster areas. Nearly all spectra have S/N greater than 10, providing radial velocity, atmospheric parameters, metallicity, and abundances of 13 other chemical elements, which greatly aids in-depth studies of cluster features and stellar evolution.

4. Completion of Observation

Within the magnitude range of *G*mag = 9–15 mag, a majority of the stars in the input catalog have been successfully observed (refer to the left side of Figure 2). This indicates that our observation plan has been effectively implemented. In the ten OCs fields, the scheduled number of stars for observation was 197,357, while the actual number of observed stars is 133,792. The completion rate has thus reached approximately 70%. Figure 2 right panel presents the histogram of the observed stars and their corresponding completeness rates within each magnitude bin in comparison to Gaia DR3. It is

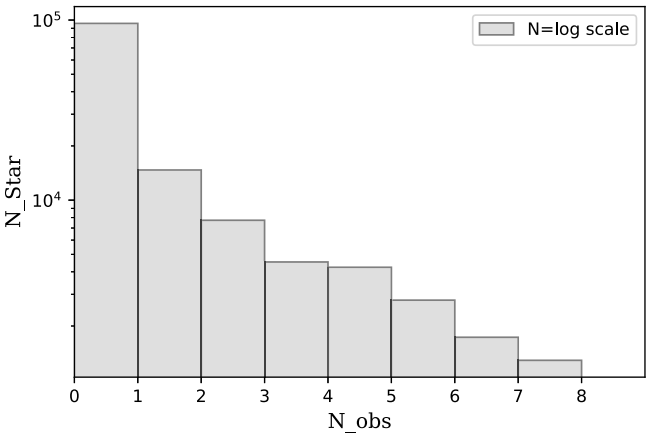

Figure 3. Distribution of the observation times of each star. The histogram indicates that the majority of stars were observed one or two times, and a small number of them were observed eight times, which is in line with the observational expectations.

evident that for stars possessing a magnitude ranging from 10 to 13 mag, the completeness rate of the observed stars can exceed 75%. Furthermore, In Figure 3, a histogram depicting the number of star observations in ten OCs fields is plotted. The majority of the stars within these areas have been observed at least 1–2 times, which is in accordance with the predefined observation strategy for the cluster areas. Regarding those stars that have been observed multiple times, their spectra can be utilized to investigate the variation of radial velocity as well as the stability of parameter measurement, thereby providing valuable insights for further astronomical research.

To further investigate the observation completion rate of cluster members, we utilized the open cluster member catalog in (Cantat-Gaudin et al. 2020) (hereafter referred to as CG20). A cross-matching process was carried out with the LAMOST-MRS-O output catalog using a radius of 3″. As a result, we obtained 2170 member stars belonging to 89 clusters. Among them, approximately 73% of the member stars, which is about 1577 in number, possess radial velocities measured by LAMOST. Figure 4 shows the histogram of the observed cluster members and their completion rate in comparison with the CG20 members in the same areas. For most clusters in this region, about 70% of the member stars with magnitudes between 10 and 13 mag have been observed.

As an example, we present the observation completeness of Stock 2 in the right panel of Figure 4. Within the magnitude range of $G = 9$–15 mag, there are 546 member stars in this cluster. Among them, 367 stars have been observed in the LAMOST-MRS-O survey. Notably, the observation completeness rate for stars with a magnitude less than 14 mag exceeds 80%. Taking into account that the fiber distribution of LAMOST is near uniform, even with eight-time sampling conducted in the cluster-dense area, some member stars may still be missed. Nevertheless, for a cluster like Stock 2, which has relatively scattered member stars, a relatively high sampling rate of its member stars can be achieved in the LAMOST-MRS-O observation mode.

5. Parameters

5.1. Radial Velocity

The LAMOST MRS general catalog offers eight distinct kinds of radial velocity measurement results along with their corresponding measurement errors. We selected rv_br1, which is obtained by combining the spectra from both the red and blue ends, as the radial velocity parameter for our sample stars. In the general catalog, a total of 235,184 combined spectra for 133,792 stars are included in ten OCs fields. From this, we selected 97,479 stars with $S/N > 10$ and rv_br_flag $= 0$. In this sample, approximately 25% of the stars have been observed twice or more times, and their average radial velocity values will be weighted according to the error of each observation. For the radial velocity and its error of a single measurement, the data provided by the LAMOST MRS general star catalog are retained.

We cross-matched the 97,479 stellar samples with the Gaia DR3 data and acquired the radial velocities of 72,737 common stars. As illustrated in Figure 5, the difference in radial velocity and its standard deviation between the LAMOST-MRS and Gaia DR3 are tiny, only $0.08\,\mathrm{km\,s^{-1}}$ and $3.09\,\mathrm{km\,s^{-1}}$ respectively. This indicates that the radial velocities of stars obtained from the LAMOST MRS spectra have high accuracy.

To inspect the average radial velocities of open star clusters, we cross-matched the stellar samples with the cluster member list of CG20. As a result, 1577 member stars in 84 star clusters were obtained, among which 77 clusters possess two or more member stars. The radial velocity and its dispersion for each star cluster are represented by the mean and standard deviation of the radial velocity values of all member stars within the cluster. After excluding the clusters with remarkably large radial velocity dispersion (exceeding $50\,\mathrm{km\,s^{-1}}$), our sample presently comprises 72 star clusters, among which seven contain only one member star. Subsequently, we discovered that there are 33 common clusters having radial velocities provided by CG20. The left panel of Figure 6 presents the comparison results of the two samples, showing a small difference and dispersion in radial velocities, which are $-2.78\,\mathrm{km\,s^{-1}}$ and $11.21\,\mathrm{km\,s^{-1}}$ respectively.

Tarricq et al. (2021) combined the spectroscopic data of Gaia DR2 (Randich et al. 2013; Sartoretti et al. 2018; Katz et al. 2019), APOGEE DR16 (Ahumada et al. 2020), RAVE DR6 (Steinmetz et al. 2020) and GALAH DR3 (Barros et al. 2020), and calculated the radial velocities of 1382 open clusters. After cross-matching with our sample, there are 57 common clusters, with radial velocity difference and dispersion of $-1.87\,\mathrm{km\,s^{-1}}$

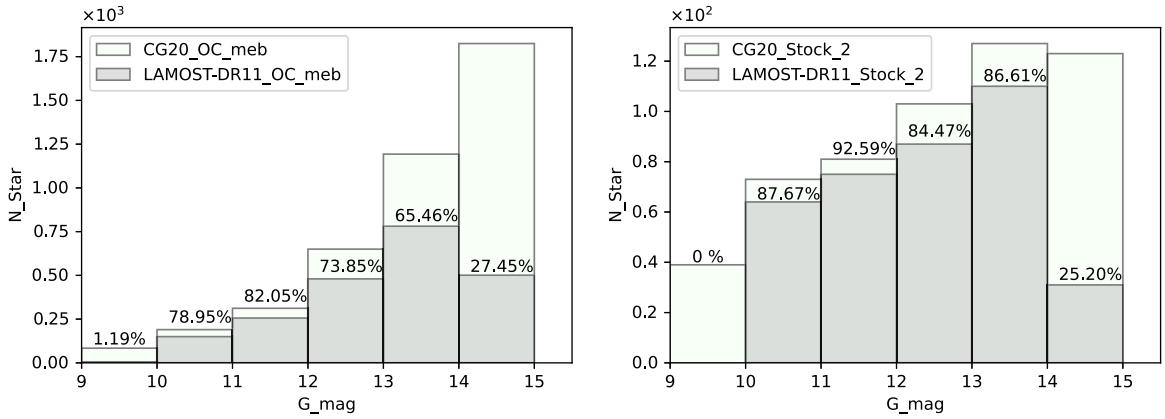

Figure 4. Distribution of the completion rate along the magnitude. The left panel presents the histogram of the observed cluster members, together with their corresponding completion rate in comparison to that of the CG20 members within the same regions. The right panel illustrates the observation completeness of Stock 2. Notably, it reveals that the observation completeness rate for stars with a magnitude brighter than 14 is greater than 80%.

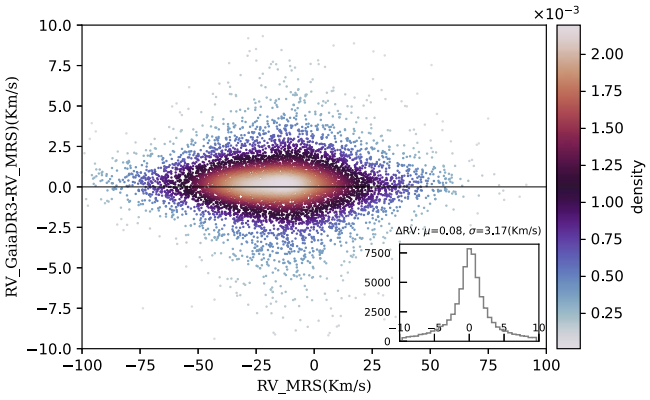

Figure 5. Difference in radial velocity between LAMOST-MRS and Gaia DR3. By calculating the radial velocity differences of 72,737 common stars, the difference value and standard deviation are only 0.08 km s^{-1} and 3.09 s^{-1} respectively.

and 14.38 km s^{-1} respectively. Refer to the right panel in Figure 6 for details.

Additionally, by making use of the LAMOST DR5 and DR8 low-resolution spectra, (Zhong et al. 2020) and (Fu et al. 2022) obtained the average radial velocities of 295 and 386 clusters, respectively. After cross-matching our sample with the tables presented in the two papers, we found 42 and 41 common clusters, respectively. The comparison differences are −5.00 km s^{-1} and −7.69 km s^{-1}, with deviations of 11.19 km s^{-1} and 9.72 km s^{-1} respectively, as illustrated in Figure 7.

In general, compared with the recent literature results, the radial velocity difference and dispersion of stars acquired through LAMOST-MRS-O exhibit relatively small values. This is essentially consistent with the conclusion proposed by (Wang et al. 2019), showing an internal accuracy of 1.36 km s^{-1} for S/N $\geqslant$ 10. It is worth noting that, in addition to the observational error, the relatively large average radial velocity dispersion within some open clusters might be attributed to the influence of binary members and the discrepant measurement errors of stars with different colors.

5.2. Metallicity

From the LAMOST-MRS DR11v1.1 stellar parameter catalog, we acquired the [M/H] abundance as well as the abundance parameters of 13 chemical elements for 67,318 stars within the ten completed observational fields. We utilized this sample to conduct an analysis on the metal abundance of targeted LAMOST-MRS-O open star clusters. Given that the LAMOST DR11v1.1 stellar parameter catalog fails to provide the observational errors of element abundances, for the stars that have been observed multiple times, their metal abundances are represented by the mean and standard deviation of the observed data. For each cluster, the average metal abundance and its associated error are signified by the mean and standard deviation of the abundances of its member stars.

The sample of 67,318 stars was cross-matched with the high-resolution APOGEE DR17, resulting in 1137 stars with [Fe/H], 904 stars with [M/H] and 968 stars with [α/M] values in common. The mean values of Δ[Fe/H] and Δ[α/M] are −0.013 dex and 0.015 dex respectively, with corresponding standard deviations of 0.025 dex and 0.012 dex. As depicted in Figure 8, the chemical abundance values provided by LAMOST-MRS are in accordance with the APOGEE results.

We further cross-matched the sample of 67,318 stars with CG20 to obtain 555 member stars belonging to 62 open star clusters. These 62 clusters were cross-matched with the literature (Zhong et al. 2020) and (Fu et al. 2022) separately, yielding 36 and 37 common clusters with [Fe/H] parameter available, respectively. The comparison results of metallicity parameters in open star clusters are shown in Figure 9. When

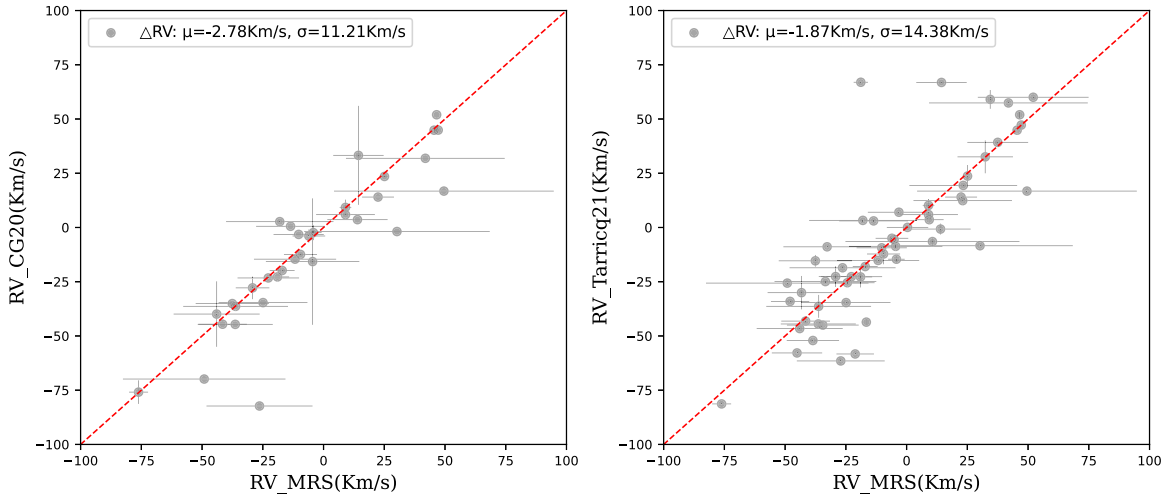

Figure 6. The left panel shows the comparison results of 33 common clusters. Their radial velocities, provided by CG20 and our sample, have small differences and dispersions, being -2.78 km s^{-1} and 11.21 km s^{-1} respectively. The right panel illustrates the differences and dispersions in radial velocities among 57 common clusters from Tarricq et al. (2021) and our samples, which are -1.87 km s^{-1} and 14.38 km s^{-1} respectively.

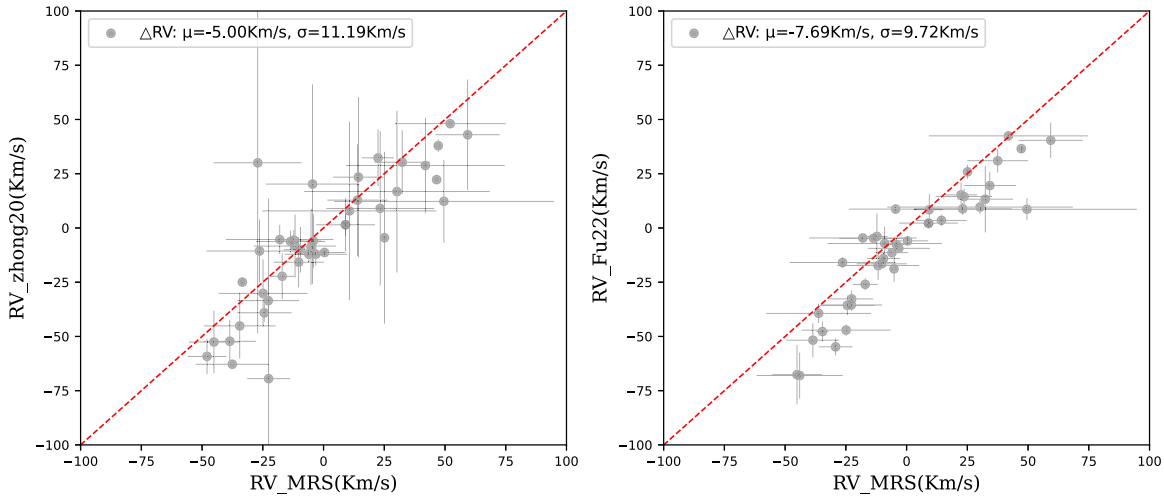

Figure 7. Comparison of radial velocity between the LAMOST low-resolution spectra results and our samples was conducted. Regarding the results from Zhong20 (with 42 common clusters) and Fu22 (with 41 common clusters), the difference results for comparison are -5.0 km s^{-1} and -7.69 km s^{-1}, respectively, whereas the deviations are 11.19 km s^{-1} and 9.72 km s^{-1}, respectively.

compared with (Zhong et al. 2020), the mean value of Δ[Fe/H] is approximately 0.002 dex and the standard derivation is around 0.121 dex, which is slightly lower than the corresponding mean difference value of approximately 0.041 dex and the standard deviation of around 0.105 dex when compared with (Fu et al. 2022).

To examine the precision of the elemental abundance results of LAMOST-MRS, we selected a cluster Stock 2 to exemplify the consistency of the elemental abundance. In the LAMOST-MRS-O survey, there are 304 member stars in Stock 2 that have spectral observations. Of these member stars, most of them provide elemental abundances, including iron, carbon, nitrogen, magnesium, silicon, calcium, nickel, etc. Table 2 lists the mean value and standard deviation of these elements in Stock 2. It can be seen that for nine abundance parameters, there are sufficient member stars in Stock 2 which have spectroscopic observations, while for the other six abundances, only two members have spectroscopic data available. In Figure 10, we plotted the metallicity distribution histograms and conducted Gaussian fittings for all the abundance

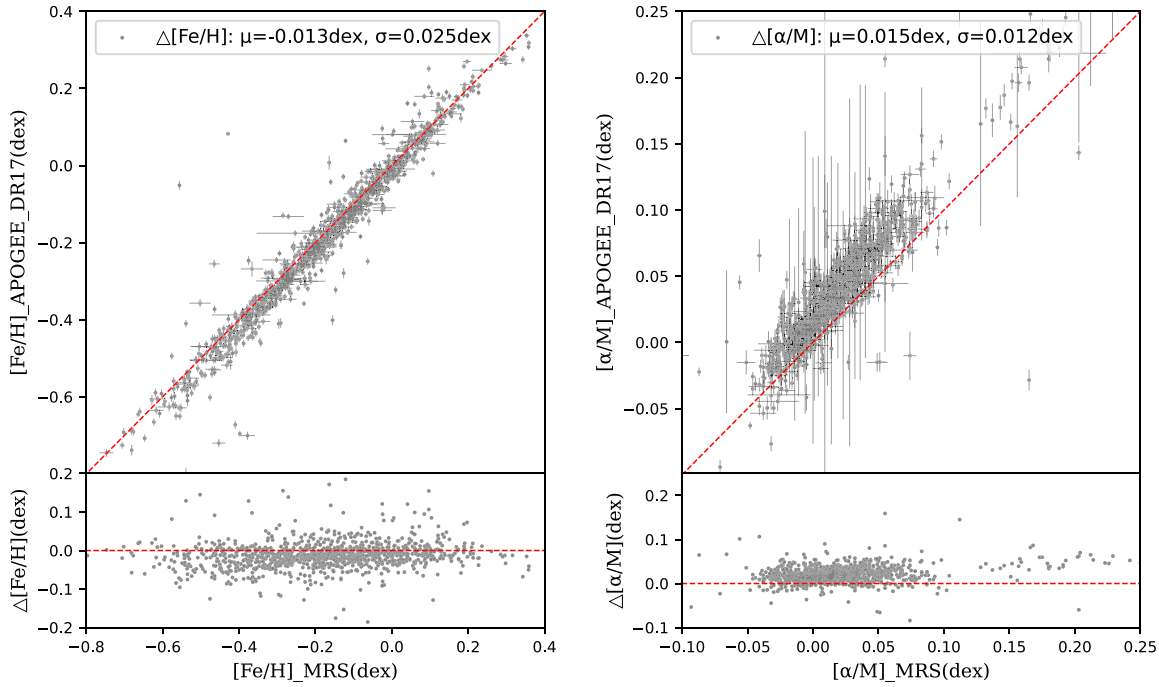

Figure 8. Comparison between APOGEE DR17 and our catalog. There are 1137 stars sharing [Fe/H] values and 968 stars sharing [α/M] values in common. The left and right panels illustrate that the mean value of Δ[Fe/H] is -0.013 dex and that of Δ[α/M] is 0.015 dex, with the standard deviations being 0.025 dex and 0.012 dex, respectively.

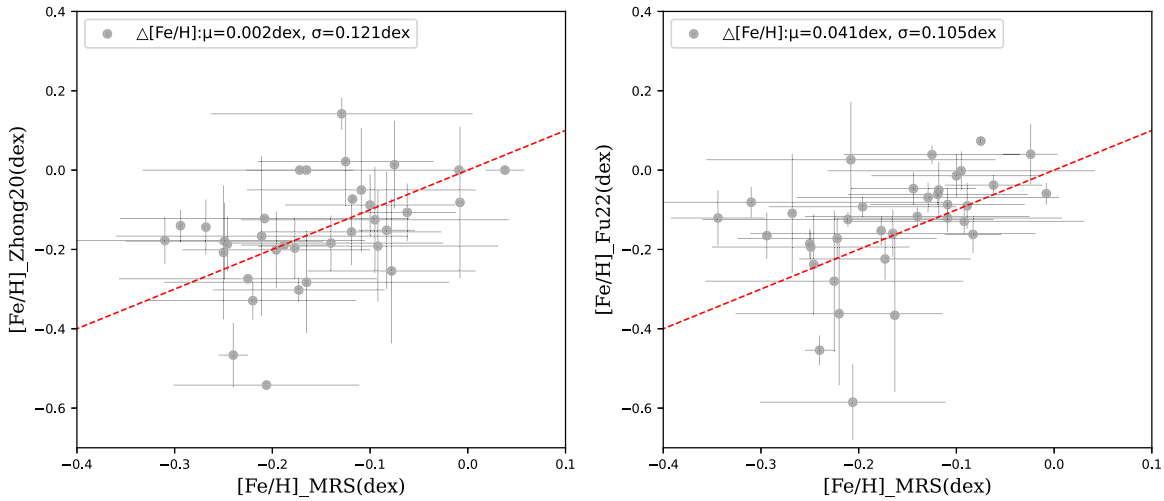

Figure 9. Discrepancies in [Fe/H] of common clusters between the literature and our samples are presented as follows. In the left panel, when they are compared with (Zhong et al. 2020), which involves 36 common clusters, the mean value amounts to approximately 0.002 dex, and the standard deviation equals approximately 0.121 dex. In the right panel, when they are contrasted with (Fu et al. 2022), which pertains to 37 common clusters, the mean value is about 0.041 dex and the standard deviation approximates to 0.105 dex.

parameters. Most abundance parameters display a good Gaussian distribution and a small standard deviation, indicating that there is no significant bias and that the LAMOST-MRS spectroscopic measurements are of high precision.

However, we observed that the distribution of the parameters exhibited an extended tail, particularly regarding the two parameters, [α/M] and [Mg/Fe]. Figure 11 shows the Stock 2 spectroscopic member distribution in the color–magnitude diagram, where colors represent the [α/M] abundance. It is clear that the extended tail of [α/M] is strongly correlated to the stellar type: the abundance measurements of hot stars tend to exhibit large deviations.

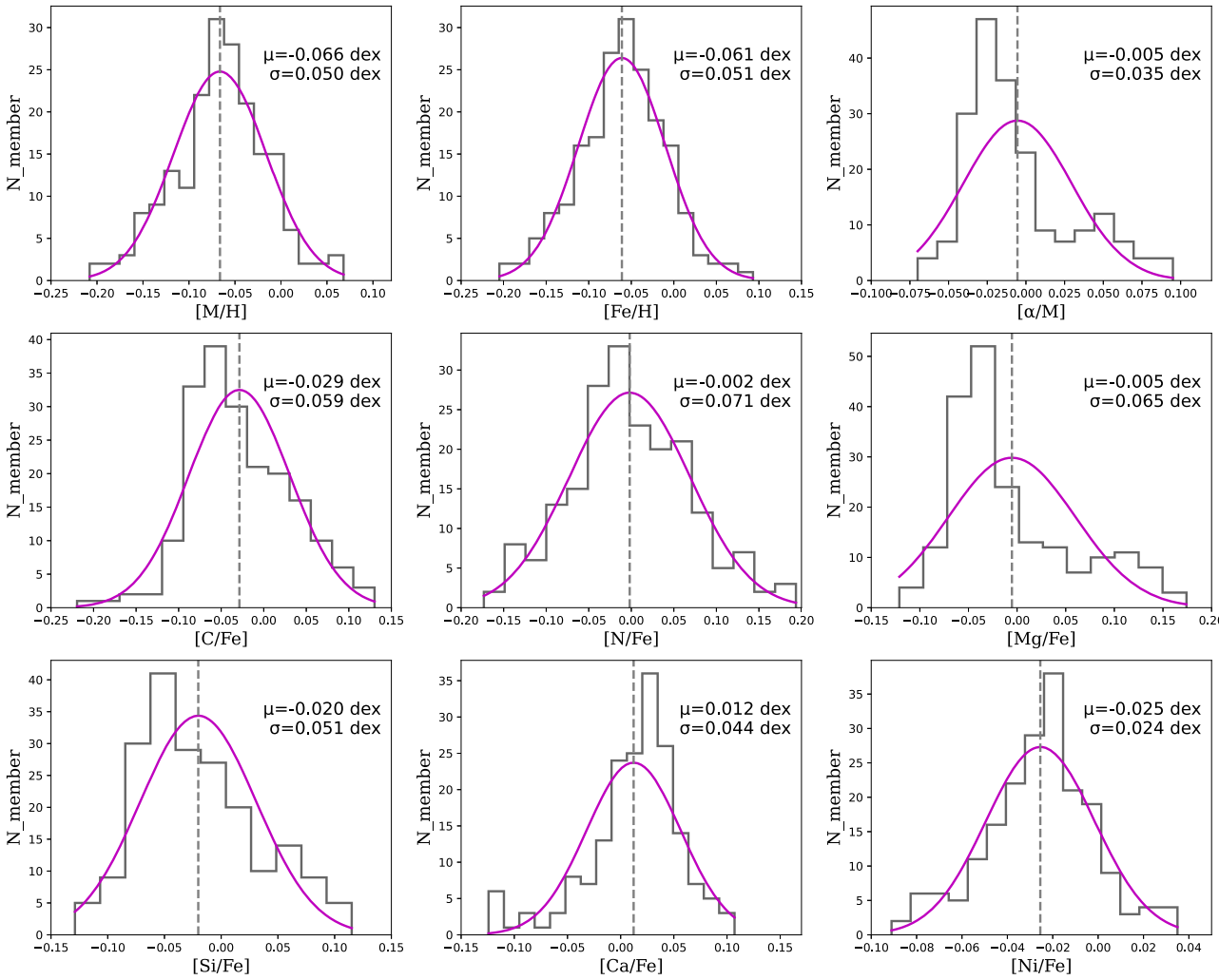

Figure 10. Histograms and Gaussian profiles for abundance parameters which have sufficient member spectra. In general, there is no significant bias and the LAMOST-MRS spectroscopic measurements are of high precision.

Table 2
Elemental Abundances of Stock 2 from the LAMOST-MRS-O Survey Data

Element	μ (dex)	σ (dex)	N_member
[M/H]	−0.066	0.050	200
[α/M]	−0.005	0.035	200
[Fe/H]	−0.061	0.051	200
[C/Fe]	−0.029	0.059	200
[N/Fe]	−0.002	0.071	200
[Mg/Fe]	−0.005	0.065	200
[Si/Fe]	−0.020	0.051	200
[Ca/Fe]	0.012	0.044	200
[Ni/Fe]	−0.025	0.024	200
[O/Fe]	0.043	0.010	2
[Al/Fe]	−0.017	0.029	2
[S/Fe]	0.063	0.031	2
[Ti/Fe]	−0.049	0.027	2
[Cr/Fe]	−0.009	0.011	2
[Cu/Fe]	0.015	0.019	2

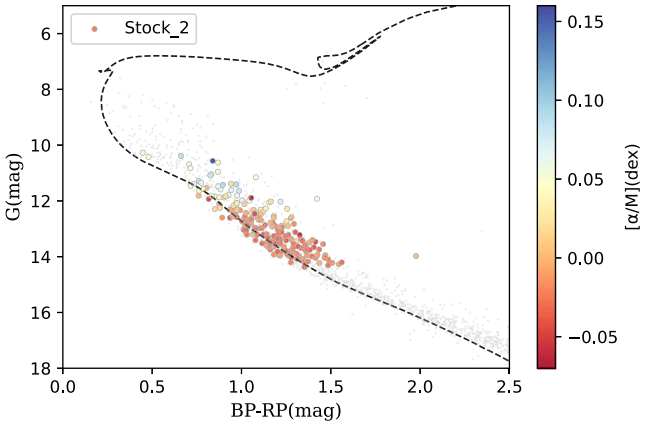

Figure 11. Spectroscopic member distribution in the color–magnitude diagram of Stock 2. Colors represent the [α/M] abundance. Moreover, the [α/M] measurements of hot stars tend to display large deviations in the LAMOST-MRS catalog.

6. Summary

We introduced the LAMOST-MRS-O survey project, which encompasses the scientific objectives, the observational plan and strategy, the observational data, as well as the completion status of the observations. The high-completeness observation mode of the LAMOST-MRS-O survey targeting over 100 Galactic open clusters is designed to acquire high-precision radial velocities, stellar parameters, and abundances of multiple elements for the cluster members. Through further integration of the distance and proper motion data from Gaia, high-precision three-dimensional spatial positions and three-dimensional velocities of the stars will be obtained, thereby significantly enhancing the reliability of cluster member determination. Additionally, by combining the multi-color photometric data of Gaia with the LAMOST spectral data of a large sample of cluster members, an effective and fully purified color–magnitude diagram can be constructed, enabling the derivation of accurate cluster ages, distances, mass distributions, and kinematic properties, which in turn provides comprehensive data support and observational constraints for stellar physics studies based on clusters.

Acknowledgments

This work is supported by the National Natural Science Foundation of China (NSFC) through grants 12090040, 12090042, and 12073060, and the National Key R&D Program of China No. 2019YFA0405501. J.Z. acknowledges the Youth Innovation Promotion Association CAS, the Science and Technology Commission of Shanghai Municipality (grant No. 22dz1202400), and the Program of Shanghai Academic/ Technology Research Leader. L.C. acknowledges the science research grants from the China Manned Space Project with NO. CMS-CSST-2021-A08. Guo Shou Jing Telescope (the Large Sky Area Multi-Object Fiber Spectroscopic Telescope LAMOST) is a National Major Scientific Project built by the Chinese Academy of Sciences. Funding for the project has been provided by the National Development and Reform Commission. LAMOST is operated and managed by the National Astronomical Observatories, Chinese Academy of Sciences.

References

Ahumada, R., Allende Prieto, C., Almeida, A., et al. 2020, ApJS, 249, 3
André, P., Arzoumanian, D., Könyves, V., et al. 2019, A&A, 629, L4
Bai, L., Zhong, J., Chen, L., et al. 2022, RAA, 22, 055022
Barros, D. A., Pérez-Villegas, A., Lépine, J. R. D., et al. 2020, ApJ, 888, 75
Bica, E., Pavani, D. B., Bonatto, C. J., et al. 2019, AJ, 157, 12
Bragaglia, A., Carretta, E., Gratton, R. G., et al. 2001, AJ, 121, 327
Cantat-Gaudin, T., Anders, F., Castro-Ginard, A., et al. 2020, A&A, 640, A1
Cantat-Gaudin, T., Jordi, C., Vallenari, A., et al. 2018, A&A, 618, A93
Carrera, R., Pasquato, M., Vallenari, A., et al. 2019, A&A, 627, A119
Castro-Ginard, A., McMillan, P. J., Luri, X., et al. 2021, A&A, 652, A162
Chen, B., Wang, S., Hou, L., et al. 2020, MNRAS, 496, 4637
Chen, L., de Grijs, R., & Zhao, J. L. 2007, AJ, 134, 1368
Chen, Y. Q., Casagrande, L., Zhao, G., et al. 2017, ApJ, 840, 77
Donor, J., Frinchaboy, P. M., Cunha, K., et al. 2020, AJ, 159, 199
Fu, X., Bragaglia, A., Liu, C., et al. 2022, A&A, 668, A4
Gaia Collaboration, Brown, A. G. A., Vallenari, A., et al. 2018, A&A, 616, A1
Hao, C. J., Xu, Y., Wu, Z. Y., et al. 2022, A&A, 668, A13
He, C., Li, C., Sun, W., et al. 2023, MNRAS, 525, 5880
He, Z., Li, C., Zhong, J., et al. 2022, ApJS, 260, 8
He, Z.-H., Xu, Y., Hao, C.-J., et al. 2021, RAA, 21, 093
Hunt, E. L., & Reffert, S. 2023, A&A, 673, A114
Hunt, E. L., & Reffert, S. 2024, A&A, 686, A42
Jiang, Y., Zhong, J., Qin, S., et al. 2024, ApJ, 971, 71
Katz, D., Sartoretti, P., Cropper, M., et al. 2019, A&A, 622, A205
Könyves, V., André, P., Men'shchikov, A., et al. 2015, A&A, 584, A91
Li, C., Sun, W., de Grijs, R., et al. 2019, ApJ, 876, 65
Li, C., Zhong, J., Qin, S., et al. 2023, A&A, 672, A81
Li, C., Zhong, J., Qin, S., et al. 2024, A&A, 686, A215
Li, L., & Shao, Z. 2022, ApJ, 930, 44
Lin, C.-C., Hou, J.-L., Chen, L., et al. 2015, RAA, 15, 1325
Lin, Z., Xu, Y., Hao, C., et al. 2022, ApJ, 938, 33
Liu, C., Fu, J., Shi, J., et al. 2020, arXiv:2005.07210
Liu, L., & Pang, X. 2019, ApJS, 245, 32
Luo, Y., Németh, P., Deng, L., et al. 2019, ApJ, 881, 7
Magrini, L., Smiljanic, R., Franciosini, E., et al. 2021, A&A, 655, A23
Maucó, K., Briceño, C., Calvet, N., et al. 2018, ApJ, 859, 1
Odenkirchen, M., Grebel, E. K., Dehnen, W., et al. 2003, AJ, 126, 2385
Pietrukowicz, P., Soszyński, I., & Udalski, A. 2021, AcA, 71, 205
Preibisch, T., Kim, Y.-C., Favata, F., et al. 2005, ApJS, 160, 401
Qin, S., Zhong, J., Tang, T., et al. 2021, RAA, 21, 045
Qin, S., Zhong, J., Tang, T., et al. 2023, ApJS, 265, 12
Rain, M. J., Ahumada, J. A., & Carraro, G. 2021, A&A, 650, A67
Rain, M. J., Carraro, G., Ahumada, J. A., et al. 2020, AJ, 159, 59
Randich, S., Gilmore, G. & Gaia-ESO Consortium 2013, Msngr, 154, 47
Romano, D., Magrini, L., Randich, S., et al. 2021, A&A, 653, A72
Röser, S., & Schilbach, E. 2019, A&A, 627, A4
Röser, S., Schilbach, E., & Goldman, B. 2019, A&A, 621, L2
Sartoretti, P., Katz, D., Cropper, M., et al. 2018, A&A, 616, A6
Sindhu, N., Subramaniam, A., & Radha, C. A. 2018, MNRAS, 481, 226
Smiljanic, R., Pasquini, L., Charbonnel, C., et al. 2010, A&A, 510, A50
Steinmetz, M., Guiglion, G., McMillan, P. J., et al. 2020, AJ, 160, 83
Sun, W., de Grijs, R., Deng, L., et al. 2019, ApJ, 876, 113
Tarasov, A. E., & Malchenko, S. L. 2012, AstL, 38, 428
Tarricq, Y., Soubiran, C., Casamiquela, L., et al. 2021, A&A, 647, A19
Wang, R., Luo, A.-L., Chen, J.-J., et al. 2019, ApJS, 244, 27
Wang, R., Luo, A.-L., Chen, J.-J., et al. 2020, ApJ, 891, 23
Zhang, Y., Tang, S.-Y., Chen, W. P., et al. 2020, ApJ, 889, 99
Zhong, J., Chen, L., Jiang, Y., et al. 2022, AJ, 164, 54
Zhong, J., Chen, L., Kouwenhoven, M. B. N., et al. 2019, A&A, 624, A34
Zhong, J., Chen, L., Wu, D., et al. 2020, A&A, 640, A127